

AD-A078 924

MISSION RESEARCH CORP SANTA BARBARA CA  
THE SENSITIVITY OF SATELLITE COMMUNICATIONS TO THE UNCERTAINTIE--ETC(U)  
MAY 79 M SCHEIBE  
DNA001-77-C-0224

F/O 20/14

UNCLASSIFIED

MRC-R-458

DNA-4971F

NL

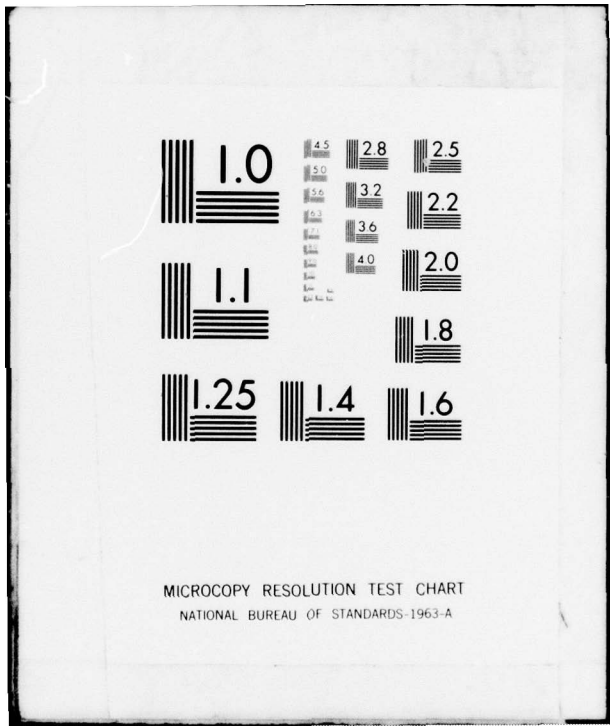
OF  
AD  
A078924



END  
DATE  
FILMED

1-80

DDC



MICROCOPY RESOLUTION TEST CHART  
NATIONAL BUREAU OF STANDARDS-1963-A

LEVEL

12

AD-E 300 633

DNA 4971F

# THE SENSITIVITY OF SATELLITE COMMUNICATIONS TO THE UNCERTAINTIES IN SELECTED CHEMICAL REACTION RATE COEFFICIENTS

AD A O 78924

Murray Scheibe  
Mission Research Corporation  
P.O. Drawer 719  
Santa Barbara, California 93102

31 May 1979

Final Report for Period April 1977-February 1979

CONTRACT No. DNA 001-77-C-0224

APPROVED FOR PUBLIC RELEASE;  
DISTRIBUTION UNLIMITED.

DDC  
RECEIVED  
JAN 8 1980  
RECEIVED  
E

THIS WORK SPONSORED BY THE DEFENSE NUCLEAR AGENCY  
UNDER RDT&E RMSS CODE B322077464 S99QAXHD41109 H2590D.

DDC FILE COPY

Prepared for  
Director  
DEFENSE NUCLEAR AGENCY  
Washington, D. C. 20305

79 11 29 009

Destroy this report when it is no longer  
needed. Do not return to sender.

PLEASE NOTIFY THE DEFENSE NUCLEAR AGENCY,  
ATTN: STTI, WASHINGTON, D.C. 20305, IF  
YOUR ADDRESS IS INCORRECT, IF YOU WISH TO  
BE DELETED FROM THE DISTRIBUTION LIST, OR  
IF THE ADDRESSEE IS NO LONGER EMPLOYED BY  
YOUR ORGANIZATION.





UNCLASSIFIED

SECURITY CLASSIFICATION OF THIS PAGE (When Data Entered)

20. ABSTRACT (Continued)

△ frequencies and some of these are significant. Areas in which improvement is needed, with regard to both reaction rate data and the chemistry treatment in MELT, are noted.

△

UNCLASSIFIED

SECURITY CLASSIFICATION OF THIS PAGE (When Data Entered)

PREFACE

We would like to thank A. W. Ali, T. Baurer, M. Bortner, and W. Swider for providing some of the reaction rate inputs. We would particularly like to thank Robert Bogusch whose inputs formed the basis of the section of communications effects.

Accession For	
NTIS G.A.I.	<input checked="" type="checkbox"/>
DLA TAB	<input type="checkbox"/>
Unannounced	<input type="checkbox"/>
Justification	<input type="checkbox"/>
By _____	
Distribution/	
Availability Codes	
Dist	Avail and/or special
A	

## CONTENTS

	PAGE
PREFACE	1
ILLUSTRATIONS	3
SECTION	
1 INTRODUCTION	5
2 REACTIONS AND RATE COEFFICIENTS	8
3 MELT CHEMISTRY RESULTS	22
4 EFFECT OF NEW RATE COEFFICIENTS AND UNCERTAINTIES	27
5 COMMUNICATION EFFECTS DUE TO CHEMISTRY VARIATION	32
6 RECOMMENDED RATE COEFFICIENTS	40
7 RECOMMENDATIONS FOR FURTHER STUDY	44

## ILLUSTRATIONS

FIGURE		PAGE
1	Rate coefficient data for reaction 16.	16
2	Rate coefficients of reaction 19 as a function of $N_2$ vibrational temperature. Kinetic temperature = 300K.	19
3	Rate coefficient of reaction 19 as a function of ion kinetic energy ( $N_2$ vibrational temperature = 298K). Kinetic temperature = $7730 \text{ KE}_{\text{cm}}$ (eV).	19
4	Relative number of reactions (compared to the total number of deionizing reactions during the 12 hour simulation) of the various chemical reactions.	23
5	Chemical reactions as a function of time after burst (2.5 minutes to 10 hours).	25
6	Total plume electron content.	28
7	Tube electron content (TEC) for central striation (Case I) and off-axis striation (Case II).	33

SECTION 1  
INTRODUCTION

During the past year or two, we have attempted to make calculations in which uncertainties in specific chemical reaction rates could be correlated to variations in UHF satellite communications degradation. Efforts to this effect using the ROSCOE nuclear weapons effects code were not successful and our attention turned to the MELT code. The MELT code was designed to describe the phenomenology following a high altitude nuclear burst out to many hours, something the ROSCOE code was not designed to do.

The degradation of UHF and higher frequency signals at high altitudes is in many ways qualitatively different from the types of degradation encountered at lower frequencies. Dispersion, diffraction, scintillation, and phase effects play a relatively more important role at high altitudes than at lower altitudes where collision induced attenuation is the dominant effect. At UHF and higher frequencies, the structure of the ionized region causing the degradation becomes an important factor. Large scale regions of ionization are known to striate at high altitudes and the spacing, amplitude, and growth rate of these striations are important parameters in calculating the effect of these regions of ionization on UHF and higher frequency signals propagating through them.

Theoretically, a variation in the chemistry parameters could impact on the growth and development of striations as well as on the overall electron density, thus having a compound effect on communications degradation. Unfortunately, the striation parameters in present high altitude

phenomenology codes are specified in an empirical manner and are not derived from other physical parameters. Under these conditions, a variation in chemistry would not impact the striation parameters and we had to content ourselves with just the effect of chemistry uncertainties on either the total electron content within the fireball or plume or the integrated electron content along a propagation path.

The reactions and rate coefficients which are in the MELT code are treated in Section 2. The relative importance of these reactions is discussed and the rate coefficient data are examined and compared with the coefficients used in MELT. The uncertainties in these rate coefficients are estimated.

Section 3 deals with the gross results of the MELT code in the area of the relative importance of specific reactions and a possibly important deficiency in the code is noted.

Section 4 deals with effect of the revised rate coefficients and their uncertainties on the plume electron content as a function of time.

Section 5 deals with variations due to the chemistry uncertainties of the tube electron content (TEC) along two hypothetical propagation paths and the effects this might have on the degradation of UHF and higher frequency communications. In order to appraise possible scintillation effects, fully developed striations were assumed.

In Section 6 we give our recommendations for the rate coefficients of the critical reactions involved in the high altitude deionization process. Reactions which are not now in MELT but possibly should be included are also discussed.

The last section deals with our recommendation for further work in the general area of high altitude nuclear induced chemistry.

SECTION 2  
REACTIONS AND RATE COEFFICIENTS

First we have the electron-ion recombination reactions



The first two reactions actually represent a complex series of processes by which an electron recombines, either by a collisional or radiative transition into a highly excited neutral atom state which is then de-excited or reionized by radiative or collisional transitions. At low electron densities, radiative processes dominate and the reaction is second order in charged particle density. At high electron densities, collisional processes dominate and the overall reaction is third order. The values used for the rate coefficient in the MELT code for  $\text{N}^+$  and  $\text{O}^+$  are shown in Table 1, where  $n_e$  is the electron density and  $T_e$  is the electron temperature in Kelvin. The rate coefficients are expressed as second order in units of  $\text{cm}^3/\text{sec}$  even when collisions dominate. These values are theoretical<sup>1</sup> and very little supportive experimental data is available. The uncertainty, however, in these values is probably fairly small, particularly when the electron density is low.

Table 1. Radiative-Collisional Rate Coefficients (in cm<sup>3</sup>/sec)

$n_e \backslash T_e$	500K	1000K	2000K	4000K	6000K
$10^7 \text{ cm}^{-3}$	4.1 E-12	1.6 E-12	7.6 E-13	3.8 E-13	2.5 E-13
$10^8 \text{ cm}^{-3}$	9.3 E-12	2.6 E-12	9.7 E-13	4.3 E-13	2.7 E-13
$10^9 \text{ cm}^{-3}$	2.7 E-11	4.8 E-12	1.4 E-12	5.1 E-13	3.1 E-13
$10^{10} \text{ cm}^{-3}$	1.1 E-10	1.2 E-11	2.3 E-12	6.7 E-13	3.6 E-13
$10^{11} \text{ cm}^{-3}$	1.0 E-9	6.1 E-11	7.1 E-12	1.5 E-12	4.0 E-13
$10^{12} \text{ cm}^{-3}$	9.0 E-9	3.6 E-10	2.5 E-11	3.1 E-12	4.0 E-13

The various dissociative recombination reactions, which is shown for  $\text{NO}^+$  in reaction 3, have rate coefficients which are many orders of magnitude faster than the radiative-collisional rate coefficients. The rate coefficient used for reaction 3 in the MELT code is

$$k_3 = \frac{1.5 \times 10^{-4}}{T_e} \text{ cm}^3/\text{sec} \quad (4)$$

Because of this large difference in the atomic and molecular recombination rates, the molecular ions formed initially disappear almost immediately relative to the atomic ions such as  $\text{N}^+$  and  $\text{O}^+$ . The long-term disappearance of the atomic ions is controlled by either radiative-collisional recombination, when the electron density is high, or reactions which convert the atomic ions to molecular ions which then disappear almost immediately relative to the remaining atomic ions. Thus, the rate controlling step, when the electron density is moderate to low, is the conversion of atomic ions to molecular ions and the values of the dissociative recombination rate coefficients are not critical. One of the reasons reaction 3, however, is important is due to the reverse reaction, i.e.,



The rate coefficient for this reaction carried in the MELT code and obtained by detailed balance is

$$k_5 = 3.6 \times 10^{-12} \exp(-31800/T_n) \text{ cm}^3/\text{sec} \quad (6)$$

where  $T_n$  is the neutral particle temperature in Kelvin. The pre-exponential factor is actually a function of temperature and the value shown is for about 5000 K. At the elevated temperatures found in the fireball or plume, reaction 5 can be an important source of ionization. In addition, reaction 3 is known to produce the excited state of atomic nitrogen,  $\text{N}(^2\text{D})$ , as a product. The presently accepted value for the fraction of the nitrogen produced as  $\text{N}(^2\text{D})$  is 0.75. If we consider  $\text{N}(^2\text{D})$  only in reaction 5, i.e.,

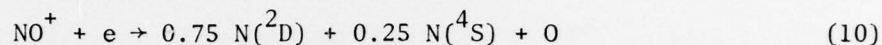


we obtain a rate constant of

$$k_7 = 3.0 \times 10^{-13} \left(\frac{T}{300}\right)^{1/2} \exp(-4300/T) \text{ cm}^3/\text{sec} \quad (8)$$

This can produce an even greater amount of ionization at even lower temperatures than reaction 5 using N in the  $^4\text{S}$  ground state. To get an appreciable effect, however, the concentration of  $\text{N}(^2\text{D})$  must be significantly larger than that at thermal equilibrium. If  $\text{N}(^2\text{D})$  is in thermal equilibrium with the ground state, then its effect is not significant and is included in the rate for reaction 5 when the total nitrogen atom concentration is used.

$N(^2D)$  is produced in nonequilibrium amounts in and near the fireball primarily from dissociative recombination of  $N_2^+$  and  $NO^+$ , i.e.,

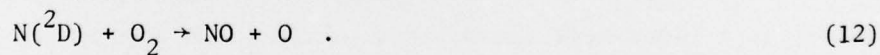


The proportions of  $N(^2D)$  produced relative to the ground state,  $N(^4S)$ , are somewhat uncertain but probably not by more than 20 percent.  $N(^2D)$  is probably produced also by the reaction

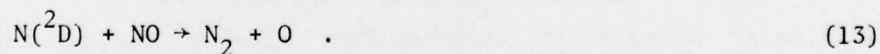


though no experimental evidence is available. This is likely because the above reaction is very nearly resonant and charge exchange reactions prefer channels which are resonant. Even in regions where the  $O_2$  is ultimately destroyed, this reaction should contribute at early times.

Whether these large nonequilibrium concentrations of  $N(^2D)$  remain over long periods of time depends in large measure on whether molecular oxygen is present in sufficient quantities to quench the  $N(^2D)$  by the reaction



The  $NO$  produced will help deplete the  $N(^2D)$  by the reaction



The rate constants for these reactions are  $7 \times 10^{-12}$  and  $6 \times 10^{-11}$   $\text{cm}^3/\text{sec}$ , respectively.

In regions where the  $O_2$  has been destroyed or is not present in sufficient quantity the quenching of  $N(^2D)$  proceeds more slowly. The quenching by electrons is fast when the electron density is large but the electron concentration may not remain large enough for enough time to significantly affect the  $N(^2D)$  depletion. The quenching rate for molecular nitrogen is small.<sup>2</sup> The rate for atomic oxygen is somewhat uncertain but is probably of the order of magnitude of  $10^{-12}$  cm<sup>3</sup>/sec.<sup>3</sup> Thus, in the region of 150 to 250 kilometers altitude the characteristic decay time for  $N(^2D)$  will be of the order of 100 to 1000 seconds. If the  $N(^2D)$  is several orders of magnitude above its equilibrium value it may take an order of magnitude longer than its characteristic decay time to reach equilibrium. Thus, under the right conditions, reaction 7 can be a significant source of ionization. This was demonstrated when the results of the high altitude chemistry model written for ROSCOE were compared to a number of benchmark calculations. In one case, that of a parcel of air at about 150 km altitude close to, but not in, the fireball, the ionization obtained over a long period of time by the ROSCOE model was significantly greater than that any of the other codes had obtained. This was due to the  $N(^2D)$ , which was carried in the ROSCOE model and allowed to deviate from equilibrium.

The experience with the ROSCOE model, however, indicated that this effect was not widespread but limited, at least during the first 10 minutes, to regions near the burst in which large amounts of  $N(^2D)$  are produced and the ambient  $O_2$  is destroyed by the energy input from the weapon. At altitudes above 200 or 250 kilometers and in the fireball, the  $O^+$  dominated the ionization to the extent that the  $NO^+$  was not significant. A systematic study of this, however, was not made.

Unfortunately, the MELT code does not carry  $N(^2D)$  as a separate species and therefore we could not assess the importance of reaction 7 at late times. In addition, MELT does not do neutral chemistry and at

80 minutes all neutral species concentrations are replaced by ambient concentrations.

Again one of the main reasons for the importance of reaction 3 is the importance of the reverse reactions, the rates of which are usually obtained from the forward rates by detailed balance. Another reason for the importance of  $\text{NO}^+$  recombination, as contrasted with  $\text{N}_2^+$  and  $\text{O}_2^+$  recombination, is due to the fact that nuclear bursts produce nitric oxide. This nitric oxide, or  $\text{NO}$ , will persist in the atmosphere for a long period of time after the bursts have occurred and after the other atmospheric species concentrations have relaxed to ambient or near ambient values. This  $\text{NO}$  can be ionized by the Lyman  $\alpha$  radiation from the sun and will increase the natural ionization in the atmosphere for long periods of time after a burst. The magnitude of this effect depends on the amount of the extra  $\text{NO}$  produced, the production rate of  $\text{NO}^+$  by Lyman  $\alpha$ , and the rate of disappearance of the  $\text{NO}^+$ . Thus the recombination rate of  $\text{NO}^+$  is also important for this reason.

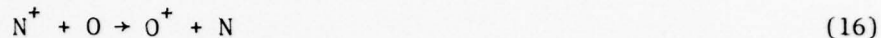
The value of the rate coefficient for  $\text{NO}^+$  dissociative recombination at 300K is fairly well established. At higher temperatures the situation is confused. Measurements in which the overall temperature was varied yield a  $T^{-1}$  dependence. Measurements in which only the electron temperature was varied yield a  $T_e^{-.4}$  dependence.<sup>4</sup> At 1000K and 3000K this amounts to factors of 2 and 4 respectively in the rate coefficient. The electron density will depend at most on the square root of the recombination coefficient and thus this does not represent a very serious uncertainty, particularly if the real values are indeed bracketed by the two temperature dependences. In addition the measurement discrepancy should be resolved within the chemical kinetics community with a reasonable amount of time.

We come now to the important exchange reactions which convert the atomic ions  $N^+$  and  $O^+$  to molecular ions such as  $O_2^+$  and  $NO^+$ . It has been consistently demonstrated in the past that in most regions these reactions are the controlling factor in the deionization process. In regions where  $O_2$  is present in sufficient quantities, the  $N^+$  will be converted to  $NO^+$  and  $O_2^+$  by the reactions



The best value at this time for the sum of the rate coefficients of these two reactions is  $6.1 \times 10^{-10} \text{ cm}^3/\text{sec.}$ <sup>5,6</sup> (Because the MELT code does not explicitly carry the species  $O_2^+$ , only reaction 15 is carried with a rate coefficient of  $5 \times 10^{-10} \text{ cm}^3(\text{sec.})$ .) The uncertainty for the total rate coefficient at 300K is small enough to be unimportant in the context of high altitude nuclear weapons effects and the dependence on temperature in the region of interest is slight. The other uncertainties regarding these reactions are in the branching ratio between reactions 14 and 15 and the amount of  $N(^2D)$  produced. An even split in the branching ratio is usually assumed though the most recent measurement<sup>5</sup> yielded 51 percent and 43 percent for reactions 14 and 15, respectively, with the remaining 6 percent going to  $O^+$  and  $NO$  as the products. The main impact of these uncertainties would be in the  $N(^2D)$  and  $NO$  production. Since  $O_2$  is present, however, subsequent reactions would yield close to the same result regardless of the specific initial channel assumed, i.e., the production of  $NO$  and three oxygen atoms. The uncertainties are, therefore, unimportant for our purpose.

In regions where molecular oxygen is not present in sufficient quantities to accommodate the  $N^+$ , such as at very high altitudes and in and near the fireball, the charge exchange reaction



is a necessary first step in neutralizing the charge. The  $\text{O}^+$  formed can then enter into reactions, to be discussed later, which yield molecular ions. Thus, if large quantities of  $\text{N}^+$  are formed, reaction 16 is of critical importance in the deionization. Of the significant reactions, reaction 16 is also the one with the greatest uncertainty. The MELT code carries a constant rate coefficient rate of  $10^{-12} \text{ cm}^3/\text{sec}$  up to a value of 0.2 eV or about 2300K for the sum of the ion and neutral temperatures. Above that the rate coefficient is taken to be a linear function of the sum of the ion and neutral temperatures. The constant rate coefficient at low temperatures is a guess. The values at high temperatures are based on an extrapolation of cross section measurements at energies of 5 eV and above. More recent experiments have extended the data down to 0.5 eV, which is much closer to the temperature regime of interest.<sup>7</sup> This data is presented in Figure 1 (circles) and is given in terms of the measured cross section,  $\sigma$ , times the relative velocity,  $v$ , of the colliding particles in the center of mass system versus the center of mass energy. The solid line represents a fit to these points between 0.5 eV and 3.5 eV energy. Though the quantity  $\sigma v$  has the dimensions of  $\text{cm}^3/\text{sec}$ , it is not, strictly speaking, a rate coefficient. However, when the fit to these values is integrated over a Maxwellian velocity distribution, we obtain a rate coefficient equal to the solid line for the temperature scale shown in Figure 1. This yields

$$k_{16} = 3 \times 10^{-13} \left(\frac{T}{300}\right) \text{ cm}^3/\text{sec} \quad (17)$$

The triangular point in Figure 1 represents a preliminary upper limit for the cross section at 0.19 eV. This value was not used in obtaining Equation 17 but is shown in order to indicate that, if true, it does not result in any inconsistency.

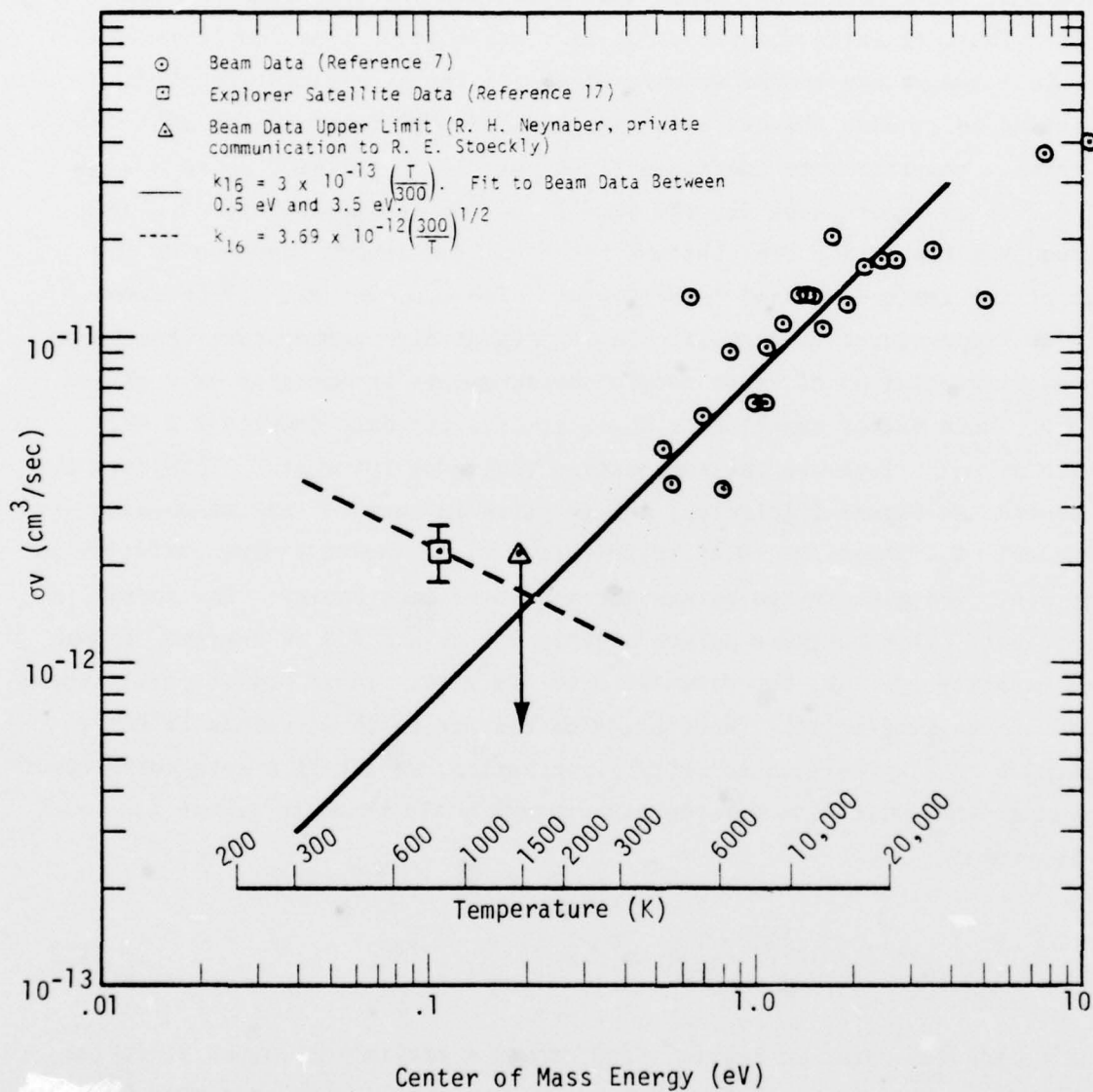
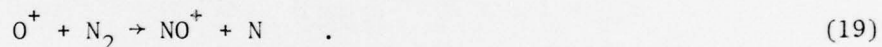


Figure 1. Rate coefficient data for reaction 16.

Equation 17 yields values for  $k_{16}$  which are within 20 percent of the values used in MELT above 800K. Because of the scatter in the data, the total uncertainty above about 4000K is easily a factor of three. Where the fit depends strongly on the extrapolation of these data values, the uncertainty increases. At 1000K, an order of magnitude or more uncertainty must be considered.\*

The  $O^+$  ion is the most important ion throughout most of the space above about 120 km, particularly if we assume the  $N^+$  can charge exchange with atomic oxygen quickly enough. In the absence of any large source of ionization,  $O^+$  will be the last ion to disappear and will thus dominate the late time ionization. The two primary reactions involving  $O^+$  are



The rate coefficient carried in the MELT code for reaction 18 is  $2 \times 10^{-11}$   $cm^3/sec$  for all temperatures. This is about the measured value at 300K<sup>5,8,9,11,14</sup> but higher temperature measurements<sup>8,9,10,11,14</sup> show a distinct decrease in the rate coefficient up to about 1800K at which point the rate coefficient is less than one-half that at 300K. The rate coefficient rises rapidly again above 1800K and at about 3000K it is  $2 \times 10^{-11}$  again. At higher temperatures, however, there is not likely to be any  $O_2$  at these altitudes so we need not be strongly concerned with the data

---

\* Very recently an analysis of the Atmospheric Explorer data has yielded a value for  $k_{16}$  of  $2.2 \times 10^{-12}$   $cm^3/sec$  at 840K with a claimed accuracy of  $\pm 20$  percent.<sup>17</sup> This value has been added to Figure 1. The dashed line represents a low temperature fit discussed in a footnote in Section 6.

above 3000K. The uncertainty is fairly small at 300K (20 percent) but because of scatter in the data, increases to about a factor of two at about 1000K.<sup>8,9,10,14</sup> This is a tolerable uncertainty if the alternate path for  $O^+$  depletion, reaction 19, is strongly dominant. If, however, reaction 18 makes up a significant, even if not dominant, fraction of the  $O^+$  depletion, this uncertainty becomes significant.

Reaction 19 is the most important reaction involved in high altitude deionization. The rate coefficient in the MELT code is, in units of  $\text{cm}^3/\text{sec}$ ,

$$\begin{aligned}
 k_{19} &= 1.2 \times 10^{-12} \left( \frac{300}{T^*} \right) & T^* < 300\text{K} \\
 k_{19} &= 1.2 \times 10^{-12} & 300\text{K} \leq T^* < 1200\text{K} \\
 k_{19} &= 1.2 \times 10^{-12} \left( \frac{T^*}{1200} \right)^2 & 1200\text{K} \leq T^* < 10000\text{K} \\
 k_{19} &= 8.26 \times 10^{-11} \left( \frac{T^*}{10000} \right) & T^* > 10000\text{K}
 \end{aligned} \tag{20}$$

where  $T^*$  is the greater of the ion temperature and the  $N_2$  vibrational temperature. This points up not only the strong dependence on translation temperature above 1200K but also the strong dependence on the vibrational state of the reacting nitrogen molecule. Figures 2<sup>12</sup> and 3<sup>8</sup> show the experimental data for  $k_{19}$  as a function of  $N_2$  vibrational temperature and translational energy. This is probably the best data available. The constant value of the rate coefficient up to about a thousand degrees nitrogen vibrational temperature (Figure 2) is attributed to the fact that the rate coefficient, at 300K translational temperature, of  $O^+$  with nitrogen in the  $v = 0$  and  $v = 1$  vibrational states is the same ( $1.2 \times 10^{-12} \text{ cm}^3/\text{sec}$ ) and the  $v = 2$  state has not been appreciably populated yet. The rapid increase in the rate constant above 1000K, when the  $v > 1$  levels progressively become populated, is taken to mean that the rate

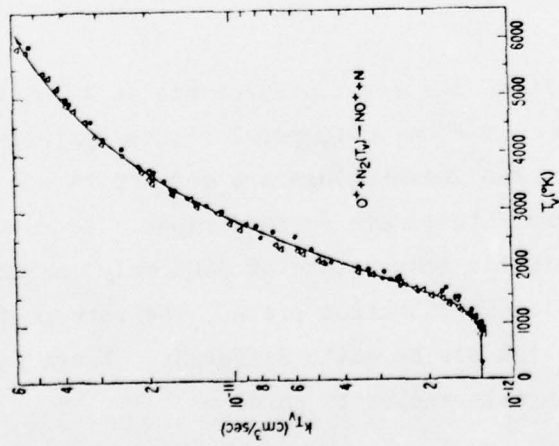


Figure 2. Rate coefficient of reaction 19 as a function of  $N_2$  vibrational temperature. Kinetic temperature = 300K.

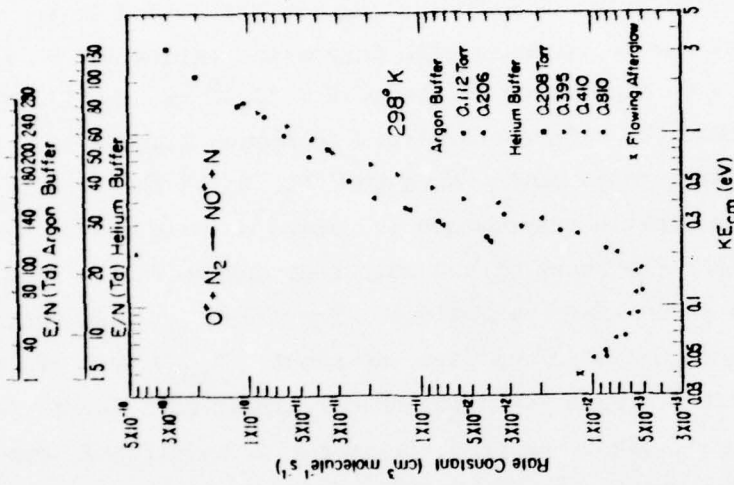


Figure 3. Rate coefficient of reaction 19 as a function of ion kinetic energy ( $N_2$  vibrational temperature = 298K). Kinetic temperature = 7730  $KE_{cm}$  (eV).

constant with  $N_2$  in the  $v = 2$  and higher levels is much larger than that for  $v = 0$  and 1. Analysis of the data in Figure 2 yields a value  $5 \times 10^{-11} \text{ cm}^3/\text{sec}$  for the reaction with the  $N_2$  in the  $v = 2$  state.<sup>12</sup> The rate constants continue to increase with increasing values of  $v$  and level off at about  $v = 6$  at a value of about  $5 \times 10^{-10} \text{ cm}^3/\text{sec}$ .<sup>12</sup> It should be emphasized that the rate coefficients in Figure 2 apply only when the translational temperature is 300K. When the  $N_2$  is in the lowest vibration state and the kinetic temperature is varied we have the situation in Figure 3. We see that the value of the rate constant decreases from its value at 300K with increasing temperature ( $T = 7730 \text{ KE}_{\text{cm}}$ ) and reaches a minimum value of about  $5 \times 10^{-13} \text{ cm}^3/\text{sec}$  at about  $\text{KE}_{\text{cm}} = 0.16 \text{ eV}$  or 1200K. In this temperature range, when the higher vibrational levels ( $v > 1$ ) of nitrogen are not significantly excited, it is the translational temperature which controls the variation of the rate coefficient. Thus, the use of a constant rate coefficient between 300K and 1200K is wrong by up to a factor of 2.4. This can be significant since the ambient temperature of the atmosphere encompasses just this range above 100 km altitude. Above 200 km altitude, the range of ambient temperature is 600K to 1200K. Thus, the rate coefficient of reaction 19 used in obtaining most of the late time MELT results is wrong by about a factor of two. We will discuss this more later.

Above about 2000K the rate coefficients as a function of nitrogen vibrational temperature and kinetic temperature are approximately the same. However, this does not mean these values are correct to use when both the ion and vibrational temperatures are in this range. To repeat, the data in Figure 2 is for a kinetic temperature of 300K only and the data in Figure 3 is only for the lowest vibration state. The rate coefficients when both temperatures are high may be quite different. There is, unfortunately, no experimental data in this regime to guide us.

Theoretical calculations have been made for the dependence of the rate coefficient as a function of both kinetic and vibrational temperatures up to 7000K.<sup>13</sup> The results agree fairly well with the data in Figure 2, when only the vibrational temperature is varied, but not too well with the data in Figure 3, when only the translational temperature is varied. The calculations are probably a good guide to the qualitative behavior of the rate coefficient when both temperatures are varied but a fairly significant uncertainty still exists quantitatively.

Another source of uncertainty is apparent in Figure 3 and applies to other rate coefficient measurements as well. The measured coefficients are different for different buffer gases (helium and argon) used in this particular set of experiments. Extrapolation of the argon data to lower energies shows significant differences down to about 600K.<sup>8</sup> The helium data more closely approximates the case for a Maxwellian speed distribution. However, the procedure of relating the ion speed distribution brought about by the application of an electric field to an effective thermal temperature introduces uncertainties, particularly when the internal excitation of the reactants plays a role in the reaction.<sup>8</sup>

Another problem is how all of the rate coefficient data is applied to a case in which the translational temperatures of the reactants are different. This is a different problem than when the translational and vibrational temperatures are different. Analysis<sup>15</sup> indicates that one may use a single translational temperature which is the mean of the translational temperatures of the reactants, each of which is weighted by the inverse of the molecular weight. For the  $O^+ + N_2$  reaction, this yields a  $T$  which is equal to  $0.64 T_i + 0.36 T_n$ . For the  $O^+ + O_2$  reaction, we have  $T = 0.67 T_i + 0.33 T_n$ , for the  $N^+ + O_2$  reaction,  $T = 0.70 T_i + 0.30 T_n$  and for the  $N^+ + O$  reaction,  $T = 0.53 T_i + 0.47 T_n$ .

### SECTION 3

#### MELT CHEMISTRY RESULTS

We shall discuss in this section two separate calculations using the MELT code. In the first case the MELT code was run for a megaton range burst at 200 km altitude to a time of about 30 minutes. The procedure beyond that time was to choose the central striation in the plume and carry it forward to about 12 hours using the MELT chemistry routines in conjunction with crude hydrodynamics.<sup>18</sup> Figure 4 contains the results of this calculation presented in a way which shows the relative importance of the different reactions we have discussed. This figure shows the number of reaction events, on a relative basis, which have taken place up to a specific time. Since the values given at any time are proportional to the integrated number of reaction events for each reaction, the slope of the curves at any given time is indicative of the relative importance of each reaction at that particular time. We see that this figure tends to contradict the assertions we made in the previous section concerning which reactions are the most important. The main bulk of the ionization is removed by the radiative recombination reactions (a reaction which results in the formation of a molecular ion is considered to be an ion removal reaction because of the rapid subsequent dissociative recombination) and up to several hours these reactions are the fastest ion removal reactions. The  $O^+ + N_2$  reaction (reaction 19) is never dominant and contributes no more than the  $O^+ + O_2$  reaction (reaction 18). This, however, is not a typical case. This calculation dealt only with the central tube or striation of the plume for a burst in which the total electron content was initially much higher than is usual. Since the radiative recombination rate depends on the square of the ion or electron density and the other

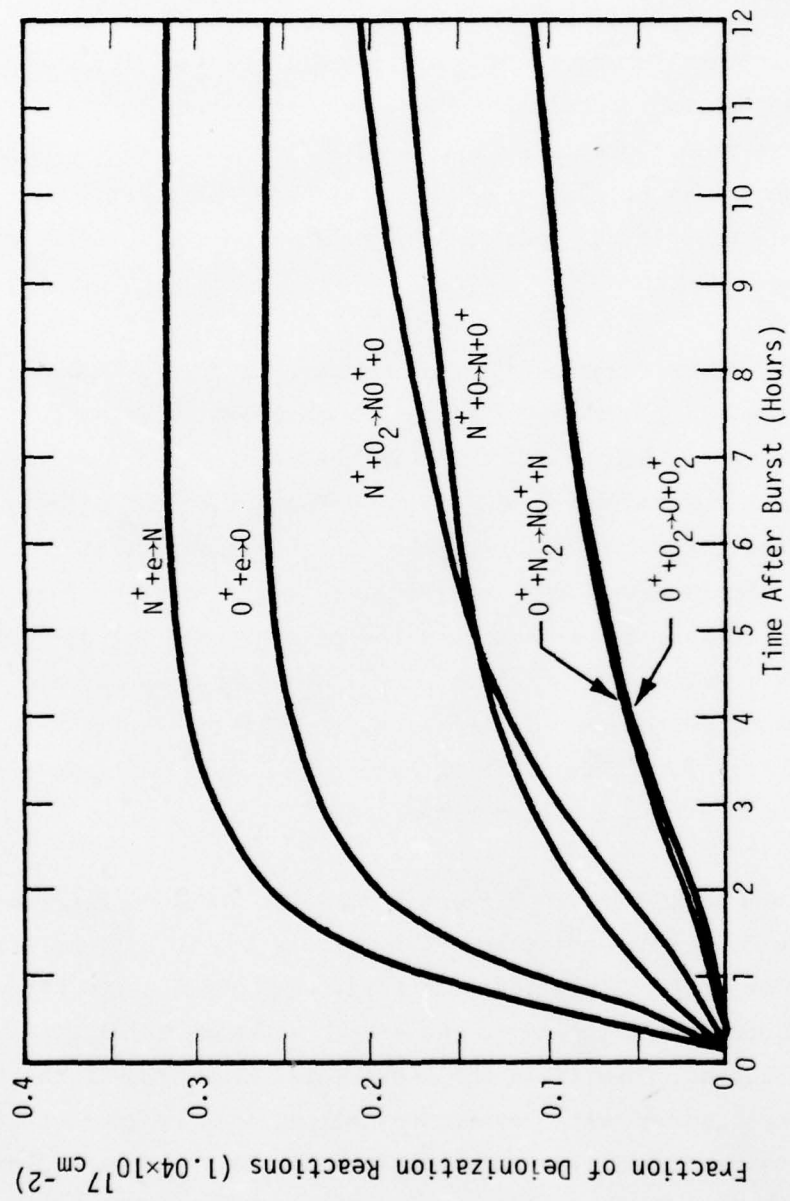


Figure 4. Relative number of reactions (compared to the total number of deionizing reactions during the 12 hour simulation) of the various chemical reactions.

reactions depend only on the first power of the ion density, the radiative recombination is enhanced relative to the ion-neutral reactions when the ionization level is high. This, however, is only part of the reason. Another reason is that because of a complicated interplay of the hydrodynamics, plasma-neutral interaction and chemistry during the time span when the tube electron content is high ( $> 2 \times 10^{16} \text{ cm}^{-2}$ ), the bulk of the electron content is held at high altitudes. At these altitudes there are very few molecules so the radiative recombination tends to be dominant in these regions.

The second calculation<sup>19</sup> gives results which we believe are more typical of the overall plume chemistry. This calculation was a full blown MELT calculation for a lower yield burst in the megaton range at 250 km altitude which was run to ten hours. Figure 5 shows information from this run similar to that in Figure 4 except that the total number of reactions are plotted and the integration is over the whole plume rather than over just the central striation. We see that the primary ion removal reaction at most times is reaction 19, which accounts for about 46 percent of all the ions removed at ten hours. In addition, the bulk of the  $\text{N}^+$  ions are depleted by reaction 16. This is in agreement with what past experience has indicated would be the important reactions.

Figure 5 shows certain discontinuities at about 80 minutes, particularly in the reactions involving  $\text{O}_2$ . This is due to a crude artifice in this particular MELT calculation, the purpose of which is to compensate for the lack of neutral diffusion in the code. At about 80 minutes, it is assumed that diffusion, were it in the code, would have brought the atmosphere back to near normal with respect to neutral species concentrations and so all neutral concentrations are replaced by their corresponding ambient concentrations. Thus, at 80 minutes, the regions in the plume which have been depleted of ambient molecular oxygen, for instance, suddenly have it replaced. There is at least one possible objection to this

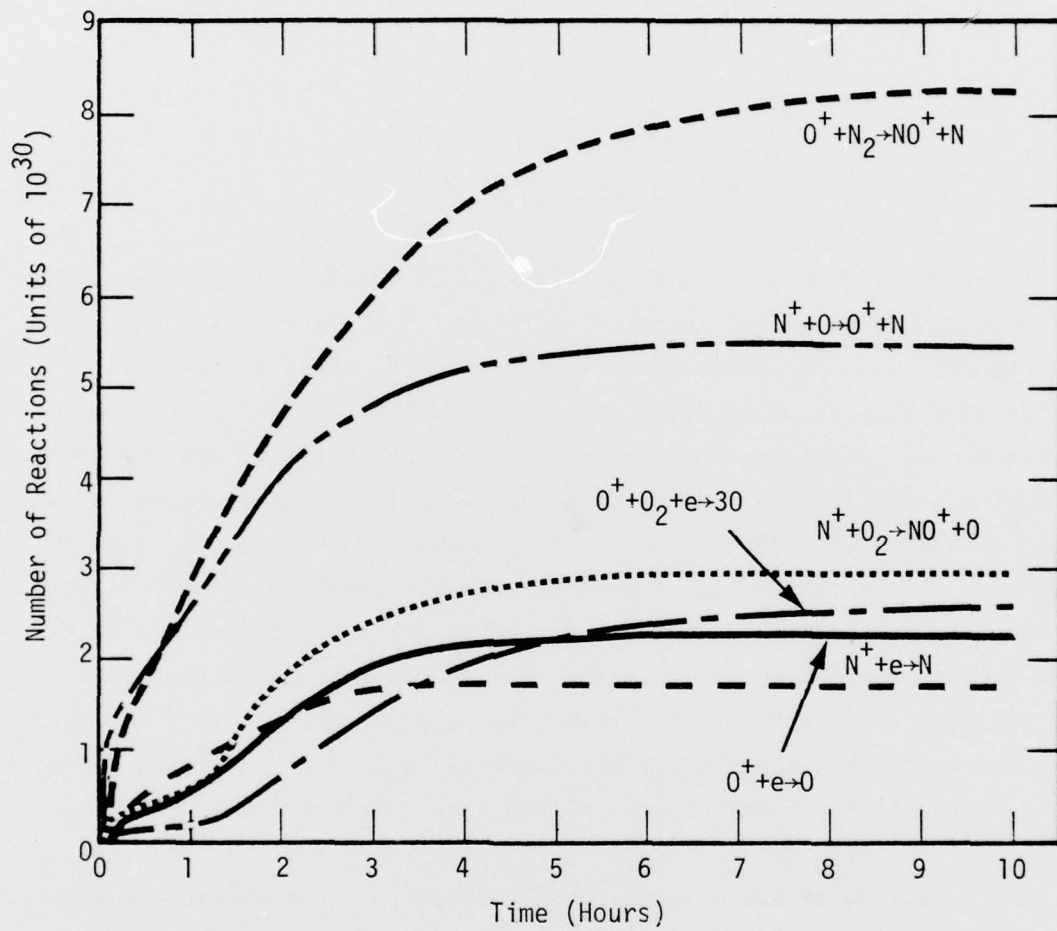
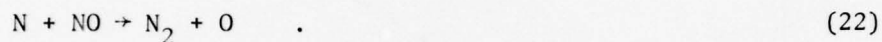
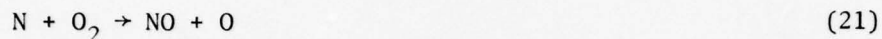


Figure 5. Chemical reactions as a function of time after burst (2.5 minutes to 10 hours).

procedure. We have discovered from calculations regarding low altitude fireballs (<100 km), in which entrainment of surrounding ambient air was included, that the initial molecular oxygen entrained was dissociated by the atomic nitrogen in the fireball. The reactions accomplishing this were



It is not until the atomic nitrogen is used up in this or other ways that the molecular oxygen concentration can build up to appreciable values. The situation in the MELT case is somewhat different as to temperature and density but the plume does contain atomic nitrogen and a certain amount of  $\text{O}_2$  diffusing into the plume would be destroyed and the process of the  $\text{O}_2$  replacement would be prolonged. This could eliminate, or at least mitigate, the enhancement of the reactions involving  $\text{O}_2$  seen in Figure 4. Since this effect would increase the amount of atomic oxygen we might expect instead an enhancement of reaction 16 ( $\text{N}^+ + \text{O} \rightarrow \text{O}^+ + \text{N}$ ). This process would also increase the NO concentrations in the plume, the possible effects of which were mentioned previously. Since the MELT code does not carry any neutral reactions as well as not carrying diffusion, it is difficult to determine how important this effect is.

Because of the assumption of ambient  $\text{O}_2$  concentrations after 80 minutes, the reactions of  $\text{O}^+$  and  $\text{N}^+$  with  $\text{O}_2$  (reactions 18, 14, and 15) become significant. Reaction 18, in fact, becomes dominant after about eight hours. It is difficult to say how significant this result is considering the discussion of the last paragraph and the fact that these reactions also tend to deplete the  $\text{O}_2$ .

## SECTION 4

### EFFECT OF NEW RATE COEFFICIENTS AND UNCERTAINTIES

In Figure 6 are plotted the MELT results for the plume total electron content (solid line) as a function of time. The altitudes and temperatures at which most of the reactions depleting the electrons are taking place are as yet largely unknown although further analysis and examination of the MELT outputs will eventually yield this information. The exponential decay time of 1.7 hours, or 6000 seconds, would indicate an altitude region of under 400 km. This is not surprising since this is where the bulk of the neutral species is located. The temperatures (the electron, ion, neutral and  $N_2$  vibrational temperatures are all likely to be different) at which the reactions are taking place are not easily estimated without further analysis of the MELT outputs. The fall of the plasma, after the initial rise, into the neutrals causes a renewed heating which may yield kinetic ion temperatures as high as  $10^4$  K. Actually, the plasma rises and falls twice before stabilizing at about 1 1/2 or 2 hours. After this time the temperatures are probably fairly close to those assumed for the ambient ionosphere. These were assumed to be 1000K for the heavy particle kinetic temperature and 1600K for the nitrogen vibrational temperature for altitudes above about 200 km.

To get some idea of what might be the effect of the different rate coefficients and uncertainties we have discussed we have used what we considered the best values for the reaction rate coefficients, and plotted in Figure 6 the electron content of the plume versus time using these values. We have assumed that the changes in the chemistry do not affect the plasma and hydrodynamic motions and we believe this is a good

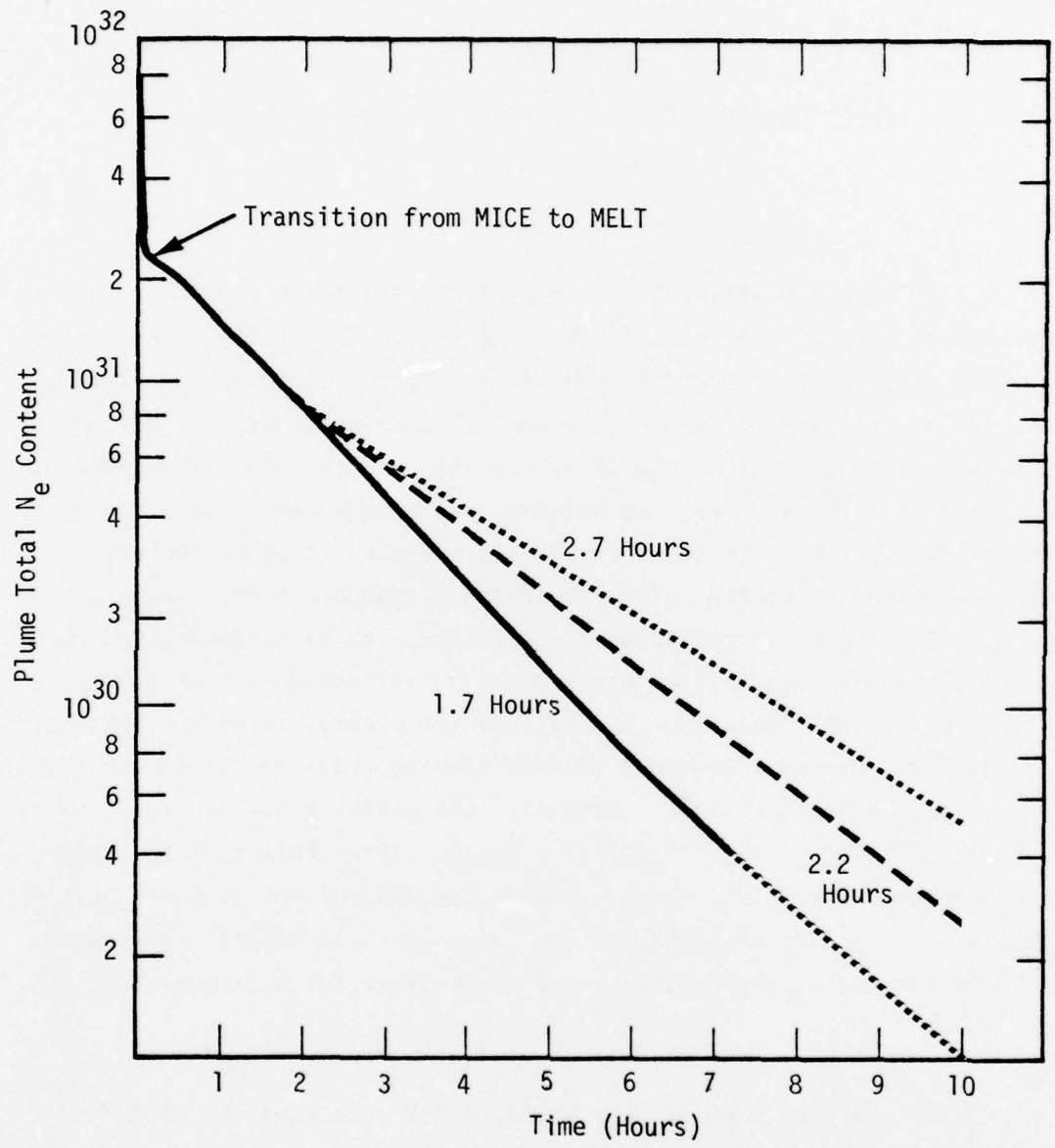


Figure 6. Total plume electron content.

5  
assumption as long as we restrict ourselves to times after the plume has stabilized. We have taken this stabilization time to be 100 minutes and have applied the new reaction rates after this time. This was a simple procedure since the total electron exponential decay time was fairly constant. As long as the ion-molecule reactions remain dominant we would expect the decay time to remain constant in time even though its value changes with changes in the rate coefficients.

With the 1600K nitrogen vibrational temperature the rate coefficient in MELT for reaction 19, the reaction of  $O^+$  with  $N_2$ , is  $2.1 \times 10^{-12} \text{ cm}^3/\text{sec}$ . The reaction we have used is based on the fact that at 1600K about 1.4 percent of the  $N_2$  is in the  $v = 2$  vibrational state, 0.2 percent in the  $v = 3$  state, and the remainder in the  $v = 1$  and  $v = 2$  states. From Figure 2, we have the rate constant for  $N_2$  in the  $v = 1$  and  $v = 2$  states, at 1000K translational temperature, is  $5 \times 10^{-13} \text{ cm}^3/\text{sec}$ . We assume that the rate constant for  $v = 2$  at 1000K is the same as at 300K, i.e., is equal to  $5 \times 10^{-11} \text{ cm}^3/\text{sec}$ . Since 1.4 percent of the  $N_2$  is in the  $v = 2$  state, we have a contribution to the overall coefficient of  $7 \times 10^{-13} \text{ cm}^3/\text{sec}$ . Similarly, the  $v = 3$  state contributes  $2 \times 10^{-12} \text{ cm}^3/\text{sec}$ . The total value is  $1.4 \times 10^{-12} \text{ cm}^3/\text{sec}$  or two-thirds of the rate coefficient used in MELT.

The value we have used for the rate coefficient of reaction 18, i.e., the  $O^+ + O_2$  reaction, at 1000K is  $10^{-11} \text{ cm}^3/\text{sec}$ . This is half the value used presently in the MELT code.

At 1000K the rate coefficient we use for reaction 16, i.e., the  $N^+ + O$  charge exchange reaction, is the same as the value used in MELT. Although this reaction does not directly produce an ion-electron recombination nor a molecular ion which can immediately recombine, it does produce much of the  $O^+$  which then feeds into reactions 18 and 19. A severe decrease in the rate coefficient of reaction 16 could cause this reaction to control, at some point, the overall rate of ion decay. An examination of Figure 5.

shows, however, that the supply of  $N^+$  is essentially depleted by about 3 to 4 hours. A severe decrease of a factor of two or more could have a significant effect and this is a possibility considering the uncertainty in this rate coefficient. A substantial increase in the rate coefficient of reaction 16, on the other hand, would have little overall effect in this case since reactions 18 and 19 are controlling the  $O^+$  ion decay.

The rate coefficients for the other reactions involved were not changed from the values in MELT. The changes in reactions 18 and 19 were enough, however, to change the exponential decay time from 1.7 hours to 2.2 hours. The effect of this on the total plume electron density is shown by the dashed line in Figure 6. At 7 hours we have a difference of about a factor of two and at 10 hours a difference of almost a factor of three.

The effect of the uncertainties in these rate coefficients can be estimated in a similar manner. We have already pointed out that the differences and scatter in the data from different experiments yields about a factor of two uncertainty in the rate coefficients as a function of kinetic temperature for reactions 18 and 19. The lack of experimental data for reaction 19 concerning the variation of the rate coefficient with kinetic temperature for the higher  $N_2$  vibrational states certainly causes at least an uncertainty of a factor of two in this contribution to the coefficient.

To these uncertainties must be added the uncertainty in reaction 16, the  $N^+ + O$  charge exchange reaction, which affects the ion decay time in an indirect way. As we mentioned before, the effect of this uncertainty will be more pronounced when the coefficient is decreased than when it is increased. A factor of two uncertainty at about 1000K either way is not unreasonable for this difficult to measure rate coefficient.

The effect of these uncertainties on the plume electron content is shown by the dotted lines in Figure 6. The electron content due to

increasing the rates coincided closely with the MELT results so this curve was used for both. These curves correspond to a 1.7 hour decay time when the rate coefficients in question are increased and to a 2.7 hour decay time when the coefficients are decreased. The fact that the effect on the electron content when the rate coefficients are decreased is less than when they are increased is due to the other reactions, whose rate coefficients are not varied. These become relatively more important in the first circumstance and limit the effect on the overall time decay constant.

SECTION 5  
COMMUNICATION EFFECTS DUE TO CHEMISTRY VARIATION

To determine the effects of the chemistry uncertainties as accurately as possible would involve running the MELT code at least twice with different rate coefficients and using the results with a communications systems code for a large number of different design parameters, frequencies and transmitter-receiver configurations. Not only would this be expensive but would not resolve the effect of  $N(^2D)$  and the lack of diffusive transport and neutral chemistry in MELT.

What we have done is to apply the uncertainties in the chemistry to two values of TEC (tube electron content) which might be encountered along a transmitter-receiver path and have tried to determine what the effects of these uncertainties would be on UHF and higher frequency communications. Many of these effects depend strongly on the type of receiver and its design parameters. We are strongly indebted to Robert Bogusch for enumerating the various communications effects, evaluating a number of these effects using realistic frequencies and design characteristics, and providing the information necessary to calculate how they would vary with variations in TEC.

The values of TEC as a function of time used were derived from the MELT results. In Figure 7 is plotted, as the first case, the TEC for the central striation (upper solid line). We have assumed that this approximates the TEC a ray path which looks up the central field line would see. Actually, because of the field line curvature this represents an upper limit for such a ray path. Ray paths probably could be found (transverse to the

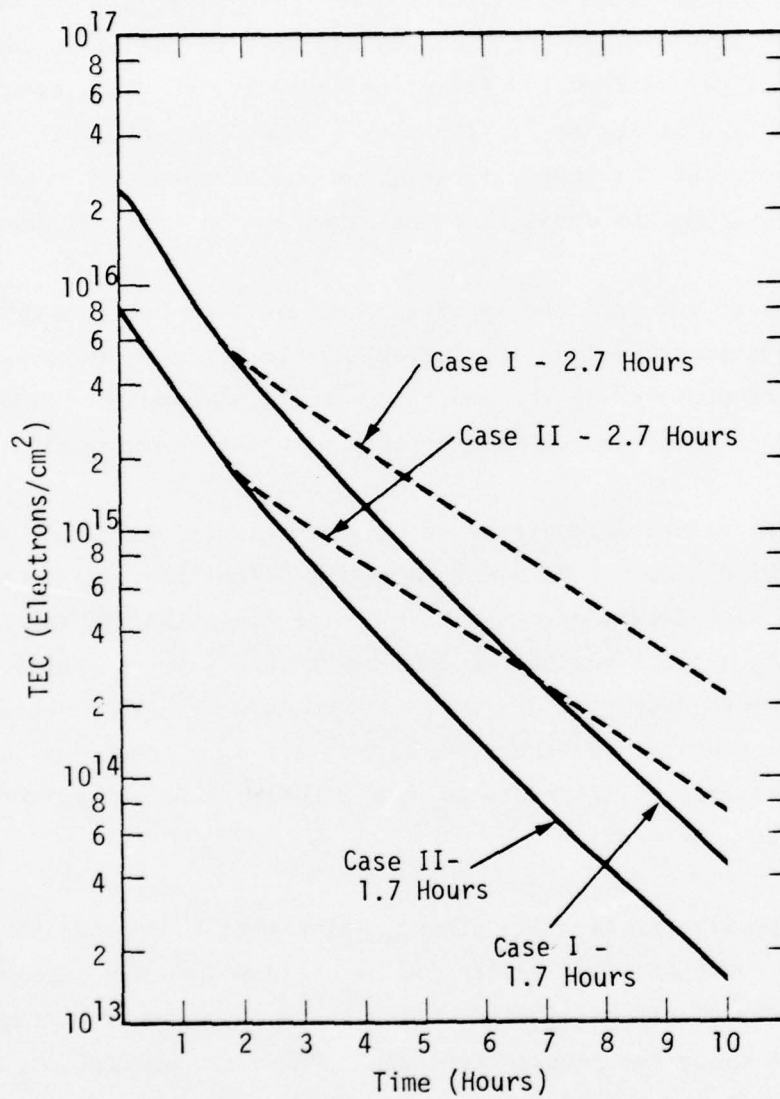


Figure 7. Tube electron content (TEC) for central striation (Case I) and off-axis striation (Case II).

plume at low altitudes), however, which would exhibit larger values of TEC. The second case was meant to approximate a ray path looking up an off-axis field line. For this average TEC a curve like that in the first case was used, but with values uniformly a factor of three lower. This is shown by the lower solid line in Figure 7. The dotted lines, together with these solid lines, represent the range of variation due to chemistry uncertainties and were plotted using the decay times obtained in the previous section.

Before we get into the specific communications effects we can examine the times these various TEC curves take to get into the range of values usually encountered in the ambient, natural atmosphere. This is an important general consideration when dealing with any communication system.<sup>16</sup>

The TEC values encountered in the natural atmosphere are in the range of  $10^{13}$  to  $10^{14}$   $\text{cm}^{-2}$ . We see from Figure 7 that the variations in chemistry cause significant uncertainties in the times the TEC takes to decrease into the ambient regime. In the first case (central tube) the variation in time to decay to  $10^{14}$   $\text{cm}^{-2}$  is about 4 hours (from about 8 1/2 hours to over 12 hours). For the second case (off-axis tube) the variation is almost 3 hours (from 6 1/2 hours to over 9 hours). Uncertainties such as these could be important.

The specific propagation effects which tend to degrade the performance of any communications system can be divided into two categories. The first category of effects include those which depend only on the mean electron content along the propagation path. These are absorption, dispersion, doppler shift and time delay rate of change. The second category includes scintillation effects which depend on the structure or degree of striation of the propagating medium. These are amplitude scintillation, phase scintillation, scintillation decorrelation time and scintillation decorrelation frequency. The estimates which follow regarding the magnitude of these effects and their variation due to our chemistry variations

are crude estimates and depend on numerous simplifying assumptions, many of which will not be explicitly stated.

The absorption,  $\alpha$ , can be expressed as

$$\alpha = \frac{1.2 \times 10^{-2}}{f^2} \int_0^{Z_T} n_e \nu_{ei} dz \quad \text{dB} \quad (23)$$

where  $f$  is the propagation frequency in Hz,  $Z_T$  is the height of the transmitter, and  $\nu_{ei}$  is the electron-ion collision frequency.  $\nu_{ei}$  is given by

$$\nu_{ei} = 1.8 n_e T^{-3/2} \ln \left( 1.2 \times 10^{16} \frac{T^3}{f^2} \right) \text{sec}^{-1} \quad (24)$$

If we take  $T = 1000\text{K}$  and  $f = 300\text{ MHz}$ , we obtain

$$\alpha = 1.5 \times 10^{-22} \int_0^{Z_T} n_e^2 dz \quad \text{dB} \quad (25)$$

Assuming the TEC is equivalent to a uniform  $n_e$  over a layer thickness of  $10^8\text{ cm}$ , we have

$$\alpha = 1.5 \times 10^{-30} (\text{TEC})^2 \quad \text{dB} \quad (26)$$

If we assume 3 dB attenuation as the criterion for significance we obtain that, for  $f = 300\text{ MHz}$ , we need

$$\text{TEC} \geq 1.4 \times 10^{15} \text{ cm}^{-2} \quad (27)$$

Examination of Figure 7 shows that, for the central striation case, the uncertainty in chemistry prolongs the time of significant attenuation from about 4 hours to 5 hours. For the off-axis striation case significant attenuation exists for about 2 hours and the chemistry uncertainty causes

only about a 15 minute effect. This last result is strongly affected by our assumption that the uncertainty in chemistry starts at 100 minutes. This was done because of our lack of specific knowledge concerning the various temperatures during the recompression phases of the motion which occurs during the first 100 minutes. There would, however, be uncertainties in the chemistry, primarily due to reaction 19, during this time. A time of 30 minutes for the prolongation of significant attenuation would probably be more reasonable for the off-axis striation case.

For L-band (1.5 GHz), a TEC of greater than  $7 \times 10^{15}$  is needed to produce significant attenuation. This means that attenuation is not a problem at this frequency except possibly at very early times.

Losses due to dispersion depend on the value of the TEC and on the modulation rate. At UHF (300 MHz), dispersive losses are negligible for any TEC below  $10^{16} \text{ cm}^{-2}$  as long as the modulation rate is less than 300 kbps, a rate in excess of any rate currently being used. At L-band (1.5 MHz) and a 10 Mbps modulation rate the dispersive loss is about 1 dB at a TEC of  $10^{16} \text{ cm}^{-2}$ . This is too small a loss to be significant. At X-band (7.5 GHz) dispersion is negligible for any TEC below  $10^{16} \text{ cm}^{-2}$  and modulation rates below 40 Mbps.

The degradations caused by doppler shift and time delay rate of change are also negligible for the cases shown in Figure 7. Thus in the first category of propagation effects, only UHF absorption is important and can be significantly affected by our chemistry uncertainties for the cases we have chosen.

In the area of scintillation effects, more assumptions are needed than in the previous category of effects to obtain any sort of quantitative results. One of these assumptions we have made is that the striations are

fully developed after two hours and the square of the electron density standard deviation is given by

$$\overline{\Delta n_e^2} = \frac{1}{4} n_e^2 = \frac{1}{4} \left( \frac{\text{TEC}}{Z_s} \right)^2 = 2.5 \times 10^{-17} (\text{TEC})^2 \quad (27)$$

where  $Z_s$ , the total thickness of the ionized layer, was again taken to be  $10^8$  cm. Another assumption is that the propagation is perpendicular to the magnetic field and thus the striations. This was assumed to make the calculations simpler although the effects in this case are less severe than when the propagation is parallel to the striations.

These simplified calculations using the TEC values in Figure 7 yield the result that, for UHF, amplitude scintillation is saturated at the Rayleigh fading limit for all values of TEC. This is true even at ambient values and the problem in this case is, as it is in the natural ionosphere, when and how the striations decay. The problem probably does not involve uncertainties in chemistry in any significant manner. The size of the region of saturated scintillation will change, however, with variations in the TEC values as a function of time.

For L-band (1.5 GHz), amplitude scintillation is saturated for 6 1/2 to 9 1/2 hours for the smaller TEC case in Figure 6 depending on the chemistry values used. For the larger TEC case the spread in time is 8 1/2 to over 12 hours. This is the same uncertainty in the time as we obtained for the TEC values to get into the ambient regime and can be considered significant.

For X-band (7.5 GHz), the analogous times are 3 to 4 hours for the lower TEC case and 5 to 7 hours for the larger TEC values. This also can be considered significant. In both the L-band and X-band, as in the UHF case, the size of the saturated region will be sensitive to chemistry.

Phase scintillation effects are directly proportional to the value of TEC thus a variation of a factor of 2 or more in TEC can translate to the same variation in the magnitude of phase scintillation. This can be important, particularly to phase coherent receivers, but quantification of system effects critically involves many receiver design parameters.<sup>16</sup>

The scintillation decorrelation time is the most important signal parameter affecting receiver performance under saturated scintillation conditions.<sup>1</sup> It varies approximately as the inverse of the value of the TEC and thus is subject to a variation of a factor of two or more after about 5 hours. This can be important to system performance but as with phase scintillation, depends critically on the system design parameters.<sup>16</sup>

The decorrelation frequency provides a measure of frequency-selective scintillation effects. When this is much less than the signal bandwidth, these frequency-selective effects can be quite important to system performance.<sup>16</sup> This is an area where investigation is currently being pursued but it can be determined that the decorrelation bandwidth varies approximately as the inverse of the TEC squared.<sup>16</sup> Thus, the variance of a factor of 2 to 5 in TEC after 5 hours due to chemistry uncertainty translates into a factor of 4 to 25 in the decorrelation bandwidth. This can be quite important to systems that use large signal bandwidths (such as GPS and DSCS spread spectrum links).<sup>16</sup>

At times greater than 5 hours, when the variation due to uncertain chemistry is greatest, X-band and higher frequency systems tend not to be scintillation saturated. Thus the sensitivity to chemistry of scintillation effects is more important for L-band and UHF systems.

To summarize the main areas where reasonable chemistry variations will affect communications, we have first that the resultant variation in times to reach ambient ionospheric conditions is significant. The times

for which signal attenuation due to ion-electron collisions is important (> 3 dB) will also vary significantly for UHF systems. The same is true for the variation in times over which we have amplitude scintillation saturation at L-band and X-band frequencies. The size of the region of scintillation saturation will probably also vary significantly with chemistry but quantification is difficult without much more analysis. Finally, during the time of scintillation saturation, important degradation effects associated with phase scintillation and scintillation decorrelation time and frequency will probably vary significantly with chemistry variations, particularly for UHF and L-band systems which are saturated to late times. These effects are critically dependent, however, on specific systems and receiver design parameters.

SECTION 6  
RECOMMENDED RATE COEFFICIENTS

The most important reaction, reaction 19, is the most difficult one for which to determine a coefficient. The problem, as indicated before, is that there is no experimental data available when both the translational and nitrogen vibrational temperatures are above about 1000K. This temperature region, however, is where most of the action takes place following high altitude bursts. We have constructed a rate coefficient based on several assumptions. The first of these is that the rate coefficients and translational temperature dependence of the nitrogen  $\nu = 0$  and  $\nu = 1$  vibrational states are identical. This probably isn't true, but is consistent with the fact that, at 300K translational temperature, the rate constant does not increase with vibrational temperature until the  $\nu = 2$  state is significantly populated. The second assumption is that the rate coefficients for the higher vibrational states are independent of translational temperature. These are taken to be  $5 \times 10^{-11}$ ,  $1.2 \times 10^{-10}$ ,  $2.5 \times 10^{-10}$  and  $4.0 \times 10^{-10}$   $\text{cm}^3/\text{sec}$ , respectively, for the  $\nu = 2$ ,  $\nu = 3$ ,  $\nu = 4$ , and  $\nu > 4$  states.<sup>12</sup> The assumption of no variation with kinetic temperature is probably not true either but seems to be the most reasonable assumption in the absence of any hard experimental data. The third assumption is that the vibrational levels in nitrogen are equally spaced. In view of the uncertainty caused by the first two assumptions, the error involved in this is trivial. Using these assumptions and some curve fitting we obtain

$$k_{19} = k_{\text{tr}} \left( 1 - e^{-6600/T_v} \right) + k_v e^{-6600/T_v} \text{ cm}^3/\text{sec} \quad (23)$$

where

$$\begin{aligned}k_{\text{tr}} &= 1.2 \times 10^{-12} \left( \frac{300}{T_{\text{tr}}} \right)^{0.7} & T_{\text{tr}} < 1200\text{K} \\k_{\text{tr}} &= 5.22 \times 10^{-13} \left( \frac{T_{\text{tr}}}{1200} \right)^{2.5} & 12000\text{K} \geq T_{\text{tr}} \geq 1200\text{K} \\k_{\text{tr}} &= 1.65 \times 10^{-10} \left( \frac{T_{\text{tr}}}{12000} \right)^{.9} & T_{\text{tr}} > 12000\text{K}\end{aligned}\quad (24)$$

and

$$k_{\text{v}} = 9.6 \times 10^{-11} \left( \frac{T_{\text{v}}}{3000} \right)^{0.8} \quad (25)$$

and  $T_{\text{v}}$  and  $T_{\text{tr}}$  are the vibrational and translational temperatures.

For reaction 16, the  $\text{N}^+ + 0$  charge exchange reaction, we have already indicated our guess, i.e.,

$$k_{16} = 3 \times 10^{-13} \left( \frac{T}{300} \right) \text{ cm}^3/\text{sec} \quad (26)$$

where  $T$  is the effective translational temperature.\*

\* More information is now available on this reaction rate coefficient. The analysis of the Atmospheric Explorer satellite data has yielded a value of  $2.2 \times 10^{-12} \text{ cm}^3/\text{sec}$  at 840K with a claimed probable accuracy of  $\pm 20$  percent. This is significantly larger than the value obtained by extrapolating the high energy data. It now appears this rate coefficient may behave as many of the other ion-molecule coefficients, i.e., first decreasing with increasing temperature and then increasing after going through a minimum. We would, therefore, now recommend (see Figure 1)

$$\begin{aligned}k_{16} &= 3.69 \times 10^{-12} \left( \frac{300}{T} \right)^{1/2} \text{ cm}^3/\text{sec} & T < 1600\text{K} \\k_{16} &= 3.0 \times 10^{-13} \left( \frac{T}{300} \right) \text{ cm}^3/\text{sec} & T \geq 1600\text{K}\end{aligned}$$

This is an increase of a factor of 2 at 1000K over the value we have used. Since we used a rather conservative uncertainty in our calculations and since, as we have pointed out, an increase in this rate would not have much of an effect at times after stabilization, our results and conclusions are not seriously affected by this new data.

For reaction 18, the  $O^+ + O_2$  charge exchange reaction, we have examined the data<sup>8,9,10,11,14</sup> and obtained

$$k_{18} = 2.1 \times 10^{-11} \left( \frac{300}{T} \right)^{0.6} \text{ cm}^3/\text{sec} \quad T < 1800\text{K}$$

$$k_{18} = 7.6 \times 10^{-13} \left( \frac{T}{300} \right)^{1.25} \text{ cm}^3/\text{sec} \quad T > 1800\text{K} \quad (27)$$

where, as before,  $T$  is the effective translational temperature.

For the sum of reactions 14 and 15 a value of  $6 \times 10^{-10}$  from 300K to 6000K is indicated by the data.<sup>9,10,11</sup> Above 6000K the rate coefficient increases with a  $T^{1/2}$  dependence.<sup>10</sup> At these high temperatures, however, there is little likelihood of  $O_2$  being present in any appreciable amount so the high temperature dependence is unimportant.

We have discussed the possibility that NO may be present in the plume in significant quantities. Unfortunately, the MELT code does not carry any of the neutral reactions and processes (e.g., diffusion) involved so it is difficult to even estimate the NO production. If, however, appreciable amounts of NO can be found, certain other ion-neutral reactions should be considered for their possible importance. Two of these reactions are



The reaction 28 rate coefficient has a value at 300K of about  $8 \times 10^{-13}$  and behaves at higher temperatures in somewhat a similar manner as the reaction 19 rate coefficient, although it does not dip down as strongly between 300K and 1200K nor rise as sharply above 1200K. Since it is highly

unlikely that the NO concentration will ever be comparable with the  $N_2$  concentration, this reaction is probably unimportant. Reaction 29, however, has a rather large rate coefficient. At 300K the value is about  $10^{-9} \text{ cm}^3/\text{sec}$  and it is unlikely that it changes significantly above 300K. Thus if the NO concentration is of the order of  $10^{-3}$  of the atomic oxygen concentration it can compete with reaction 16 at ambient temperatures and directly convert  $N^+$  to a molecular ion.

Another reaction which must be considered is



Analysis of the Atmospheric Explorer satellite data<sup>17</sup> has yielded a value of  $1.3 \times 10^{-10}$  for the rate coefficient of reaction 30 and it is claimed that this reaction is important in the natural ionosphere.<sup>17</sup> What the effect would be in the nuclear disturbed case is difficult to ascertain. If the  $N(^2D)$  concentration is within two orders of magnitude of the  $N_2$  concentration, the  $O^+$  will be converted more rapidly to  $N^+$  by reaction 30 than to  $NO^+$  by reaction 19. This would tend to slow the total ion decay and to make reactions 14, 15, and 16 (the reactions of  $N^+$  with  $O_2$  and O) relatively more important than we have assumed.

## SECTION 7

### RECOMMENDATIONS FOR FURTHER STUDY

The obvious recommendation would be to reduce the rate coefficient uncertainties which have been determined to be important. The problem is that one of the reasons these uncertainties still persist long after their importance was recognized is the extreme difficulty in doing experiments under the conditions of interest. Reaction 16, the  $N^+ + O$  charge exchange reaction, which is important at all altitudes within the plume below about 500 km, is a case in point. The interesting region is from 0.5 eV energy down to thermal energies. The measurements, however, do not go below 0.5 eV and these were not easy to obtain and have been accomplished only recently. Fortunately, the decrease in the rate coefficient of reaction 19 at ambient conditions below what was used in the MELT code makes it more improbable that reaction 16 will control the total ion decay at any time after plume stabilization. A decrease of two or three in the rate coefficient of the  $N^+ + O$  reaction at 1000K from the value obtained by extrapolating the experimental values would be needed to make this reaction the controlling factor. Since the extrapolation involves a range in temperature of a factor of 4 rather than the factor of 40 we had prior to the recent measurements, this large a decrease in the rate coefficient, though possible, is not very likely. At times prior to stabilization, when the ion temperature may be as high as 1 eV, the  $O^+ + N_2$  reaction goes much faster than at ambient temperature and the  $N^+ + O$  reaction will probably be the rate controlling reaction, particularly since the  $O_2$  is depleted and diffusion certainly has not had time to replace it. At these higher energies we are, however, in or very near the range of the experimental data. The uncertainty, therefore, is less than in the region of the data extrapolation. It would

7

be reassuring to have experimental data in the region of 0.1 and 0.5, particularly at the low end of this energy range,\* but this is not of the highest priority. The uncertainty in reaction 18, the  $O^+ + O_2$  charge exchange reaction, which is important below about 350 km altitude, has been shown to have some measure of importance. This importance is not as great as the importance in the uncertainty in reaction 19 except possibly at very late times. In addition, this uncertainty stems largely from the scatter in the data from a number of experiments. Assuming all the experiments are equally reliable, which they are not, a reduction in this uncertainty would involve doing a large number of further experiments. Finally, this uncertainty is probably overshadowed by uncertainties introduced by the lack of  $O_2$  diffusion and neutral chemistry in the plume. For these reasons reducing the uncertainties in the rate coefficient of reaction 18 is also not of the highest priority.

The uncertainty in the rate coefficient of reaction 19, which is important at all altitudes up to 500 km, is the most important uncertainty we have discussed. This is the rate controlling reaction for total ion decay and occurs at temperatures not encompassed by the experimental data. It is of high priority to measure this rate coefficient when both kinetic and  $N_2$  vibrational temperatures are above 1000K. In particular, measurements which would reveal the dependence on kinetic temperature of the rate coefficient for the reaction when  $N_2$  is in the  $v = 1, 2,$  and  $3$  vibrational states would be extremely useful.

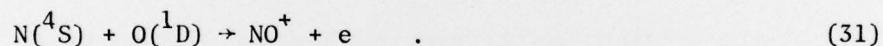
The uncertainty of  $N(^2D)$  depends strongly on the uncertainties in the excited state production in the initial energy deposition phase, the production by electron impact during the recompression phases of plume development, and the quenching by atomic oxygen. The quenching is particularly

---

\* The AE satellite data analysis has yielded a value of  $2.2 \times 10^{-12} \text{ cm}^3/\text{sec}$  at 840K.<sup>17</sup>

important and of high priority. If the quenching rate coefficient is of the order of  $10^{-11}$ , the effect of  $N(^2D)$  will be restricted to only the first minute or two after its production, either initially or during plume recompression, and thus not very important to communications. If the rate coefficient is of the order of  $10^{-12}$  or less, the effect of  $N(^2D)$  might be important to communications for times of the order of an hour after production. A measurement of this rate coefficient is therefore of high priority.

In this respect, subsidiary questions arise. When  $N(^2D)$  is quenched by atomic oxygen, is an  $O(^1D)$  state produced? Also, when  $NO^+$  dissociatively recombines, is an  $O(^1D)$  produced in the channel where the nitrogen is produced in the  $N(^4S)$  state? If the answers to both of these are yes, then we may have to worry about the reaction



Quenching of  $O(^1D)$  by  $N_2$ , which has a rate coefficient of about  $3 \times 10^{-11} \text{ cm}^3/\text{sec}$ ,<sup>4</sup> as well as a small rate coefficient for reaction 31, probably makes this unimportant. However, a large production of  $O(^1D)$ , and its subsequent quenching by  $N_2$ , which results in  $N_2$  vibrational excitation, could substantially affect the  $N_2$  vibrational distribution. This would impact strongly on the value of the rate coefficient of reaction 19. Further investigation is needed, but it would be useful if the amount of production of  $O(^1D)$  for the  $N(^2D)$  quenching reaction were measured as well as the value of the rate coefficient.

A further possible effect of  $N(^2D)$  stems from the reaction



which, according to the Explorer satellite data analysis, has a fairly large rate coefficient. The effect of this reaction on the total ion decay should be investigated.

The last uncertainty we have discussed is that involved in the depletion of  $O_2$  in and near the plume, its replacement by diffusion, and the mitigation of its replacement due to neutral reactions involving atomic nitrogen. This impacts not only on all ion reactions involving  $O_2$  but on the production of NO, whose presence and persistence could substantially alter the ambient ionosphere for very long periods of time after a number of high altitude bursts. This could involve important communications effects and should be investigated.

## REFERENCES

1. Sappenfield, D., Radiation from a Recombining Oxygen Plasma, LA-4303 Supplement, February 1971.
2. Black, G., et al., JCP 51, 116 (1969),  
Lin, C., and F. Kaufman, JCP 55, 3760 (1971).
3. Davenport, J. E., et al., JGR 81, 12 (1976).
4. DNA Reaction Rate Handbook, DNA 1948H.
5. Smith, D., et al., JCP 69, 308 (1978).
6. Lindinger, W., et al., JGR 79, 4753 (1974).
7. Rutherford, J. A., and R. H. Neynaber, Measurements of Selected Charge Transfer Processes at Low Energies, DNA 4695F, November 1978.
8. Albritton, D. L., et al., JCP 66, 410 (1977).
9. Lindinger, W., et al., JGR 79, 4753 (1974).
10. McFarland, M., et al., JCP 59, 6620 (1973).
11. Dunkin, D. B., et al., JCP 59, 1365 (1968).
12. Schmeltekopf, A. L., et al., JCP 48, 2066 (1968).
13. Van Zandt, T. E., and T. F. O'Malley, JGR 78, 6818 (1973).
14. Chen, A., et al., JCP 69, 2688 (1978).
15. Stoeckly, R. E., et al., DNA 3827T.
16. Bogusch, R. L., private communication.
17. Dalgarno, A., AE Reaction Rate Data, AFGL-TR-79-0067, March 1979.
18. Kilb, R. W., and Chavin, S., private communication.
19. Fajen, F. E., Gregersen, A. W., Kilb, R. W., Stoeckly, R. E., and White, W. W., private communication.

## DISTRIBUTION LIST

### DEPARTMENT OF DEFENSE

Assistant to the Secretary of Defense  
Atomic Energy  
ATTN: Executive Assistant

Defense Advanced Rsch. Proj. Agency  
ATTN: TIO

Defense Documentation Center  
12 cy ATTN: DD

Defense Nuclear Agency  
ATTN: DDST  
2 cy ATTN: RAAE  
4 cy ATTN: TITL

Field Command  
Defense Nuclear Agency  
ATTN: FCPR

Field Command  
Defense Nuclear Agency  
Livermore Division  
ATTN: FCPRL

Interservice Nuclear Weapons School  
ATTN: TTV

Undersecretary of Defense for Rsch. & Engrg.  
ATTN: Strategic & Space Systems (OS)

### DEPARTMENT OF THE ARMY

Atmospheric Sciences Laboratory  
U.S. Army Electronics R&D Command  
ATTN: DELAS-EO-MO, M. Heaps  
ATTN: DELAS-EO, F. Niles  
ATTN: DELAS-EO-ME, K. Ballard

BMD Advanced Technology Center  
Department of the Army  
ATTN: ATC-O, W. Davies  
ATTN: ATC-T, M. Capps

Harry Diamond Laboratories  
Department of the Army  
ATTN: DELHD-N-P  
ATTN: DELHD-I-TL

U.S. Army Ballistic Research Labs.  
ATTN: DRDAR-BLB, M. Kregel  
ATTN: DRDAR-BLP, J. Heimerl  
ATTN: DRDAR-TSB-S

U.S. Army Foreign Science & Tech. Ctr.  
ATTN: DRXST-SD-3

U.S. Army Missile R&D Command  
ATTN: Redstone Scientific info. Ctr.

U.S. Army Nuclear & Chemical Agency  
ATTN: Library

U.S. Army Research Office  
ATTN: R. Mace

### DEPARTMENT OF THE ARMY (Continued)

U.S. Army TRADOC Systems Analysis Activity  
ATTN: ATAA-PL

White Sands Missile Range  
Department of the Army  
ATTN: STEWS-TE-AN, M. Squires

### DEPARTMENT OF THE NAVY

Naval Electronic Systems Command  
ATTN: ELEX 03  
ATTN: Code 501A  
ATTN: PME 117-20

Naval Intelligence Support Ctr.  
ATTN: Document Control

Naval Ocean Systems Center  
ATTN: Code 4471  
ATTN: Code 5321, I. Rothmuller  
ATTN: Code 532, J. Richter  
ATTN: Code 5324, W. Moler  
ATTN: Code 532, R. Pappert  
ATTN: Code 5322, H. Hughes

Naval Postgraduate School  
ATTN: Code 0142, Library

Naval Research Laboratory  
ATTN: Code 7120, R. Kinzer  
ATTN: Code 7175, J. Johnson  
ATTN: Code 1434, E. Brancato  
ATTN: Code 2627  
ATTN: Code 6750, K. Hain  
ATTN: Code 6709, W. Ali  
ATTN: Code 7175H, D. Horan  
ATTN: Code 6701, J. Brown  
ATTN: Code 6780, S. Ossakow  
ATTN: Code 6750, D. Stobel  
ATTN: Code 7101, P. Mange  
ATTN: Code 6780, J. Fedder  
ATTN: Code 7122, D. McNutt  
ATTN: Code 6700, T. Coffey  
ATTN: Code 7750, J. Davis

Naval Surface Weapons Center  
ATTN: Code F31  
ATTN: Code F46, D. Hudson  
ATTN: L. Rudlin  
ATTN: Code R41, D. Land

Nuclear Weapons Tng. Group, Pacific  
Department of the Navy  
ATTN: Nuclear Warfare Department

Office of Naval Research  
ATTN: Code 421, B. Junker  
ATTN: Code 465, G. Joiner

### DEPARTMENT OF THE AIR FORCE

Air Force Weapons Laboratory, AFSC  
ATTN: SUL  
ATTN: DYV, E. Copus

DEPARTMENT OF THE AIR FORCE (Continued)

Air Force Geophysics Laboratory

ATTN: SULL  
ATTN: PHG, F. Innes  
ATTN: OPR-1, J. Ulwick  
ATTN: LKB, E. Murad  
ATTN: LKB, J. Paulson  
ATTN: LKB, K. Champion  
ATTN: LKD, R. Narcisi  
ATTN: LKB, T. Keneshea  
ATTN: LKB, W. Swider, Jr.  
ATTN: LKD, C. Philbrick  
ATTN: LKO, R. Van Tassel  
ATTN: LKO, R. Huffman  
ATTN: OP, J. Garing  
ATTN: OPR, T. Connolly  
ATTN: OPR, J. Kennealy  
ATTN: OPR, F. Delgreco  
ATTN: OPR, H. Gardiner  
ATTN: OPR, R. O'Neill

Air Force Technical Applications Center

ATTN: TD  
ATTN: STINFO Office  
ATTN: TF, L. Seiler

Foreign Technology Division

Air Force Systems Command

ATTN: NIIS, Library  
ATTN: WE

Rome Air Development Center

Air Force Systems Command

ATTN: OCSA, J. Simons  
ATTN: OCS, V. Coyne

USAFETAC

Department of the Air Force

ATTN: CBTL, STOP 825

OTHER GOVERNMENT AGENCIES

Bureau of Mines

Pittsburgh Mining & Safety Rsch. Ctr.

ATTN: J. Murphy

Department of Commerce

National Bureau of Standards

ATTN: S. Leone  
ATTN: W. Lineberger  
ATTN: A. Phelps

Department of Commerce

National Bureau of Standards

ATTN: J. Cooper  
ATTN: J. Devoe  
ATTN: M. Scheer  
ATTN: D. Garvin  
ATTN: D. Lide  
ATTN: M. Krauss  
ATTN: R. Hampson, Jr.  
ATTN: S. Abramowitz  
ATTN: L. Gevantman

Department of Commerce

National Oceanic & Atmospheric Admin.

ATTN: J. Angell  
ATTN: L. Machta

OTHER GOVERNMENT AGENCIES (Continued)

Department of Commerce

National Oceanic & Atmospheric Admin.

ATTN: Assistant Administrator, RD

Department of Commerce

National Oceanic & Atmospheric Admin.

ATTN: D. Albritton  
ATTN: F. Fehsenfeld  
ATTN: W. Spjeldvik  
ATTN: G. Reid

Department of Transportation

Transportation Rsch. System Center

ATTN: F. Marmo

NASA

Goddard Space Flight Center

ATTN: J. Vette  
ATTN: A. Aikin  
ATTN: Code 625, M. Sugiura  
ATTN: S. Bauer  
ATTN: Code 625, J. Heppner  
ATTN: Technical Library

NASA

George C. Marshall Space Flight Center

ATTN: W. Roberts

NASA

ATTN: R. Schiffer  
ATTN: N. Roman  
ATTN: E. Schmerling

NASA

Johnson Space Center

ATTN: Code JM6, Technical Library

NASA

Ames Research Center

ATTN: N-245-3, R. Whitten  
ATTN: W. Starr

National Science Foundation

ATTN: R. Sinclair  
ATTN: Div. of Atmos. Sci., R. McNeal

DEPARTMENT OF ENERGY CONTRACTORS

Lawrence Livermore Laboratory

ATTN: Document Control for L-71, J. Chang  
ATTN: Document Control for L-262, W. Duerer

Los Alamos Scientific Laboratory

ATTN: Document Control for MS 212,  
W. Barfield  
ATTN: Document Control for MS 664, J. Zinn  
ATTN: Document Control for MS 668, J. Malik  
ATTN: Document Control for MS 560, W. Hughes  
ATTN: Document Control for MS 668, H. Hoerlin  
ATTN: Document Control for MS 362, Librarian

Sandia Laboratories

ATTN: Document Control for Org. 4241,  
T. Wright  
ATTN: Document Control for Org. 1250,  
W. Brown

DEPARTMENT OF DEFENSE CONTRACTORS

Aerodyne Research, Inc.  
ATTN: M. Camac  
ATTN: Librarian, B. Duston  
ATTN: M. Faist  
ATTN: F. Bien

Aerospace Corp.  
ATTN: Library  
ATTN: M. Whitson  
ATTN: T. Taylor  
ATTN: R. Cohen  
ATTN: H. Mayer

University of Alaska  
ATTN: Technical Library  
ATTN: N. Brown  
ATTN: R. Parthasarathy

AVCO Everett Research Lab, Inc.  
ATTN: C. Von Rosenberg, Jr.

Berkeley Research Associates, Inc.  
ATTN: J. Workman

Boston College  
ATTN: Chairman, Dept. of Physics  
ATTN: Science Library, F. McElroy  
ATTN: Dept. of Chemistry, D. McFadden

University of California at San Diego  
ATTN: D. Miller

University of California at Santa Barbara  
ATTN: M. Steinberg

California Institute of Technology  
ATTN: V. Anicich  
ATTN: S. Trajmar

Calspan Corp.  
ATTN: W. Wurster  
ATTN: Library  
ATTN: C. Treanor

University of Colorado  
ATTN: Dept. of Chemistry, V. Bierbaum

EG&G, Inc.  
ATTN: Document Control for J. Colvin  
ATTN: Document Control for P. Lucero  
ATTN: Document Control for D. Wright

ESL, Inc.  
ATTN: W. Bell

General Electric Co.  
ATTN: Technical Information Center  
ATTN: P. Zavitsanos  
ATTN: J. Burns  
ATTN: M. Linevsky  
ATTN: J. Peden  
5 cy ATTN: T. Baurer  
6 cy ATTN: M. Bortner

General Electric Co.  
ATTN: J. Schroeder

DEPARTMENT OF DEFENSE CONTRACTORS (Continued)

General Electric Company-TEMPO  
ATTN: M. Dudash  
ATTN: D. Reitz  
ATTN: D. Chandler  
ATTN: DASIAC  
ATTN: J. Thompson  
ATTN: L. Ewing  
ATTN: B. Gambill  
ATTN: M. Stanton  
ATTN: T. Stevens  
ATTN: W. Knapp

General Research Corp.  
ATTN: J. Ise, Jr.

General Research Corp.  
ATTN: T. Zakrzewski

HSS, Inc.  
ATTN: D. Hansen  
ATTN: M. Shuler

Institute for Defense Analyses  
ATTN: E. Bauer  
ATTN: H. Wolfhard

IRT Corp.  
ATTN: R. Overmyer  
ATTN: D. Vroom  
ATTN: R. Neynaber  
ATTN: J. Rutherford

Johns Hopkins University  
ATTN: Document Librarian

Kaman Sciences Corp.  
ATTN: D. Foxwell  
ATTN: W. Rich

Harold W. Lewis

Lockheed Missiles and Space Co., Inc.  
ATTN: R. Sears  
ATTN: J. Reagan  
ATTN: M. Walt  
ATTN: J. Kumer  
ATTN: J. Evans  
ATTN: B. McCormac  
ATTN: R. Gunton  
ATTN: T. James

M.I.T. Lincoln Lab.  
ATTN: B. Watkins

Mission Research Corp.  
ATTN: M. Messier  
ATTN: V. Van Lint  
ATTN: M. Scheibe  
ATTN: D. Sappenfield  
ATTN: R. Kilb  
ATTN: R. Hendrick  
ATTN: W. White  
ATTN: D. Archer  
5 cy ATTN: Document Control

DEPARTMENT OF DEFENSE CONTRACTORS (Continued)

National Academy of Sciences  
ATTN: J. Sievers

Nichols Research Corp., Inc.  
ATTN: R. Tippets

Pacific-Sierra Research Corp.  
ATTN: E. Field, Jr.

Pennsylvania State University  
ATTN: J. Nisbet  
ATTN: L. Hale

Photometrics, Inc.  
ATTN: I. Kofsky

Physical Dynamics, Inc.  
ATTN: A. Thompson

Physical Science Lab.  
ATTN: W. Berning

Physical Sciences, Inc.  
ATTN: K. Wray  
ATTN: R. Taylor  
ATTN: G. Caledonia

University of Pittsburgh  
ATTN: W. Fite  
ATTN: F. Kaufman  
ATTN: M. Biondi

R&D Associates  
ATTN: R. LeIevier  
ATTN: R. Turco  
ATTN: B. Gabbard  
ATTN: H. Ory  
ATTN: C. MacDonald  
ATTN: F. Gilmore

R&D Associates  
ATTN: H. Mitchell  
ATTN: J. Rosengren  
ATTN: B. Yoon  
ATTN: R. Davidson

Rand Corp.  
ATTN: C. Crain

DEPARTMENT OF DEFENSE CONTRACTORS (Continued)

Science Applications, Inc.  
ATTN: D. Hamlin

Science Applications, Inc.  
ATTN: N. Byrn  
ATTN: D. Divis  
ATTN: R. Deliberis

Science Applications, Inc.  
ATTN: R. Johnston

SRI International  
ATTN: E. Kindermann  
ATTN: V. Wickwar  
ATTN: A. Peterson  
ATTN: M. Baron  
ATTN: R. Hake, Jr.  
ATTN: G. Black  
ATTN: J. Peterson  
ATTN: A. Whitson  
ATTN: J. Moseley  
ATTN: R. Leadabrand  
ATTN: D. Hildenbrand  
ATTN: T. Slanger

SRI International  
ATTN: C. Hulbert

University of Texas System  
ATTN: J. Browne

TRW Defense & Space Sys. Group  
ATTN: Technical Information Center  
ATTN: J. Frichtenicht

Utah State University  
ATTN: K. Baker

Visidyne, Inc.  
ATTN: O. Manley  
ATTN: C. Humphrey  
ATTN: T. Degges  
ATTN: H. Smith  
ATTN: J. Carpenter